Environmental Technology & Innovation 41 (2026) 104739

Contents lists available at ScienceDirect

Environmental Technology & Innovation

journal homepage: www.elsevier.com/locate/eti

Coffee pulp and husk-derived hydrochars and biochars adsorb polyphenols and pesticides from wastewater

Brigitte Mukarunyana [a,c], Cecilia Sundberg [e], Christoffer Boman [b], Telesphore Kabera [d], Jerker Fick [a,*]

[a] Department of Chemistry, Faculty of Science and Technology, Umeå University, Umeå SE-901 87, Sweden
[b] Department of Applied Physics and Electronics, Umeå University, Umeå SE-901 87, Sweden
[c] Department of Chemistry, College of Science and Technology, University of Rwanda, PO Box 3900, Kigali, Rwanda
[d] School of Engineering, College of Science and Technology, University of Rwanda, PO Box 3900, Kigali, Rwanda
[e] Department of Energy and Technology, Swedish Agricultural University, 75007 Uppsala, Sweden

ARTICLE INFO

Keywords:
Coffee Processing Wastewater Treatment
Hydrochar and Biochar Adsorption
Polyphenol Removal
Pesticide Adsorption
Coffee Byproduct Valorization

ABSTRACT

Coffee processing generates significant amounts of wastewater rich in organic compounds and sometimes also pesticides. This poses environmental challenges for producing regions. This study aimed to assist coffee producers by providing local waste management solutions by examining the adsorption efficiency of hydrochars and biochars derived from coffee pulps (CP) and coffee husks (CH) in removing polyphenols and pesticides from coffee processing wastewater (CPWW). These materials were tested for the adsorption of selected polyphenols and pesticides from CPWW. Hydrochars exhibited high removal efficiencies for polyphenols (up to 100 %), primarily via hydrogen bonding, while biochars effectively adsorbed hydrophobic pesticides (removal efficiencies up to ~75 %) through hydrophobic interactions. Adsorption data fitted the Freundlich isotherm, indicating multilayer adsorption, and kinetic analyses suggested complex mechanisms involving both physisorption and chemisorption. These findings demonstrate the potential of coffee waste-derived chars to serve as sustainable adsorbents for mitigating pollution from CPWW, offering a promising local waste management strategy in coffee-producing countries

1. Introduction

Coffee is one of the most extensively traded commodities in the global market and the cultivation of coffee constitutes a major global agricultural sector, with approximately 80 countries participating in its large-scale production and exportation (Hoseini et al., 2021; Murthy and Madhava Naidu, 2012). Ten billion kilograms of coffee are consumed annually globally (ICO, 2023). The coffee tree, a long-lived plant from the *Rubiaceae* family, produces a fruit with distinct layers. A fully mature coffee fruit has a vibrant red outer layer (epicarp) that encases the distinctly pectic mucilage (mesocarp). This is followed by a delicate parchment-like layer known as the endocarp, and finally, the last layer, called silverskin, that envelops the coffee bean (Esquivel and Jimenez, 2012; Hoseini et al., 2021; Murthy and Madhava Naidu, 2012). To obtain the final coffee product, ripe coffee cherries undergo an extensive post-harvest processing sequence designed to separate the coffee beans from the surrounding pulp, mucilage, and outer layers (Iriondo-DeHond et al., 2020). Coffee fruits can be processed using either the wet or dry methods. The wet method has gained popularity, and many coffee

* Corresponding author.
E-mail address: jerker.fick@umu.se (J. Fick).

https://doi.org/10.1016/j.eti.2025.104739
Received 2 November 2025; Received in revised form 15 December 2025; Accepted 30 December 2025
Available online 9 January 2026

producers utilise it to meet the market demand for higher-quality green coffee beans (Poltronieri and Rossi, 2016). It is standard procedure in regions like Central and South America, East Africa, and certain areas of Asia (Alves et al., 2017; Esquivel and Jimenez, 2012; Iriondo-DeHond et al., 2020; Murthy and Madhava Naidu, 2012; Pandey et al., 2000). In the wet process, coffee fruits are sorted and cleaned with water, and the epicarp layers are mechanically removed, generating coffee pulp (CP) as a byproduct. Depulped beans are placed into fermentation tanks filled with water, where they ferment for 24–72 h (Esquivel and Jimenez, 2012). During this fermentation stage, naturally occurring enzymes decompose the remaining mesocarp, a honey-like substance that adheres to the beans (Da Mota et al., 2020). After fermentation, the beans are washed extensively with water to remove any remaining mucilage (Figueroa Campos et al., 2020; Vinícius de Melo Pereira et al., 2017). The cleaned coffee beans are dried and then sent to mills for hulling. This involves separating the coffee beans from the dried endocarp layer. Hulling is followed by dry milling, which entails removing the seed's silverskin (Alves et al., 2017). In the dry method, the harvested fruits are dried and then dehusked (Arya et al., 2022).

Processing coffee generates a lot of waste; estimates show that almost 90 % of coffee fruits generate byproducts, primarily CP and Coffee husks (CH) (Alemayehu et al., 2021). In addition, approximately 40–45 litres of coffee processing wastewater (CPWW) are generated for every kilogram of coffee beans produced when using the wet method (Esquivel and Jimenez, 2012; Zayas Péerez et al., 2007). CPWW is characterized by a high biochemical oxygen demand (BOD) of 14,200 mg/L, a chemical oxygen demand (COD) of 25, 600 mg/L, and total suspended solids (TSS) of 5870 mg/L, along with a low pH range of 3–4 (Alemayehu et al., 2021; Zayas Péerez et al., 2007). CPWW are also rich in carbohydrates, minerals, proteins, and other organic compounds such as tannins, caffeine, and phenolics, which can affect plants and aquatic life (Amare et al., 2023; Ameca et al., 2018). Similarly, CP and CH disposed of in the environment emit unpleasant odours caused by phenols, methane and hydrogen sulfide from degradation (Genanaw et al., 2021; Laili et al., 2022). In addition, pesticide residues may be washed out with CPWW during the depulping and washing steps (Merhi et al., 2022). Pesticides are regularly applied at various stages of coffee cultivation to reduce and prevent diseases that impact production, quality, and quantity (Leite et al., 2020; Merhi et al., 2022; Taghizadeh et al., 2022). De Queiroz et al. revealed that 44.7 % of surface water and 23.7 % of groundwater were contaminated with pesticides used in coffee farming in Brazil (De Queiroz et al., 2018).

Although no established guidelines for the management of CPWW have been established, significant progress has been achieved in its treatment, management, and valorization strategies (Tsigkou et al., 2025). Chemical treatments, including advanced oxidation processes (AOP) like photocatalysis with oxygen, peroxide H_2O_2 and Fe^{2+} (Ameta et al., 2018), as well as UV catalysis with ozone or ozonation (Takashina et al., 2018), have been applied to generate strong oxidants for organic compounds present in CPWW. However, studies have reported that these methods require adequate pH control and high consumption of hydrogen peroxide (Villanueva-Rodríguez et al., 2014; Yamal-Turbay et al., 2012). Electro-oxidation (Ibarra-Taquez et al., 2017) and coagulation-flocculation methods have also been employed (Asefaw et al., 2024; Rattan et al., 2015). Biological methods like activated sludge, anaerobic and aerobic methods, enzymes, etc., have been investigated (Hailemariam et al., 2021; Ijanu et al., 2019; Tsigkou et al., 2025). Although they efficiently removed BOD and COD, they did not remove colour and acidic components (Alemayehu et al., 2020; Ijanu et al., 2019). Different researchers have discussed the adsorption method in water and wastewater treatment (Dutta et al., 2021; Satyam and Patra, 2024). Activated carbon has been widely utilized as an adsorbent in water purification owing to its large surface area, porous structure and strong affinity for organic compounds (Dutta et al., 2021; Heidarinejad et al., 2020). Nonetheless, activated carbon has certain disadvantages, including its high cost, low selectivity and challenges in regeneration (Heidarinejad et al., 2020; Satyam and Patra, 2024). As a complement, alternative adsorbents have been investigated, including silica gel, metal oxides, polymers, and several types of carbonaceous materials, for use in wastewater treatments (Satyam and Patra, 2024). These adsorbents offer various characteristics and benefits compared to activated carbon, including greater adsorption capacity, enhanced selectivity, improved stability, reduced cost and better recyclability (Dutta et al., 2021; Lawal et al., 2021; Singh et al., 2021). Especially carbonized materials such as biochars and hydrochars produced during pyrolysis and hydrothermal carbonization (HTC) (Khan et al., 2019; Tangmankongworakoon, 2019), respectively, are among the most promising adsorbents used in wastewater treatment. They have been applied to remove organic and inorganic pollutants from aqueous solutions and in the soil to increase its fertility as soil amendments (Bona et al., 2023; Tan et al., 2015).

Rwanda, an Eastern African country with a surface area of 22,338 km^2 and a population of about 13.2 million (NISR, 2023) has cultivated coffee since the beginning of the 20th century. Coffee is primarily grown by small-scale farms with an average of 165 coffee trees per farmer (NAEB, 2024). Currently, there are 245 coffee washing stations (CWS), of which 216 are operational. Many hectares of plantations continue to be added, averaging 42,429 ha (NAEB, 2024). Coffee byproducts are often poorly managed, resulting in their decomposition or incineration in open areas or being disposed of near those stations. Despite a growing number of coffee producers, awareness of the benefits of carbonizing coffee byproducts and applying biochar and hydrochars in coffee waste management remains limited and proper treatment of CPWW is lacking. Few, if any, studies have been conducted on this subject matter in Rwanda, examining the impact of CPWW on one side and CP and CH on the other side on the environment, particularly on the nearest water bodies, to assess the extent of the problem and suggest solutions and recommendations accordingly.

This study aimed to produce biochar and hydrochar from coffee pulps and husks using pyrolysis and hydrothermal carbonization techniques. Subsequently, it intended to utilise these carbonised materials as adsorbents to remove organic compounds and pesticides from wastewater generated during coffee processing at a washing station in Rwanda. As adsorption typically involves various mechanisms, this study investigated the behaviour and mechanisms at play during the adsorption of organic compounds and pesticides using the produced biochars and hydrochars. Finally, various kinetic and isothermal models were formulated to detail the kinetics and adsorption equilibrium, providing further insights into the adsorption mechanisms involved.

2. Materials and methods

2.1. Chemicals

This study includes polyphenols, including caffeic (CAF) and ferulic acids (FEA), as well as catechin (CAT), which are naturally occurring organic compounds in coffee. The pesticides examined in the study were a subset of those most commonly utilised in coffee cultivation: Acetamiprid (ACE), Azoxystrobin (AZO), Carbendazim (CRB), Cyproconazole (CYP), Dimethoate (DIM), Imidacloprid (IMD), Metalaxyl (MET), Tebuconazole (TEB), and Triadimefon (TRI). Fig. 1 illustrates the molecular structures of all the compounds included in this investigation. Physicochemical properties are displayed in Table S1 of the Supplementary Materials. Internal and pesticide standards were designated as analytical grade (>95 %). Stock solutions for each pesticide were prepared using methanol and stored at −18°C.

The methanol or acetonitrile used for standard solutions was of HPLC quality and sourced from Fisher Chemicals in Loughborough, UK. Hypergrade methanol (LiChrosolv) intended for LC-MS applications was obtained from Merck in Darmstadt, Germany. Formic acid (Fluka), used as an eluent additive, was acquired from Sigma-Aldrich in Steinheim, Germany. A Merck Millipore Advantage A10 system with Q-Pod unit equipment provided ultrapure water.

2.2. Preparation of hydrochars and biochars

Biochars and hydrochars were produced from two types of feedstock, coffee pulp (CP) and coffee husk (CH). These feedstocks were collected from one washing station in Rwanda and transported to Umeå University, where the biochars and hydrochars were produced. Pyrolysis and hydrothermal carbonization were used to prepare the biochars and hydrochars, respectively. To prepare hydrochars, the feedstock was placed in a small reactor with Milli-Q water added to facilitate hydrothermal carbonization (HTC). For 5 g of coffee pulps and coffee husks, 5 ml and 20 ml of water were added, respectively. The reactor was then tightly closed and placed in a Nabertherm muffle furnace B410, made in Germany, for carbonization. Two temperatures were used to produce hydrochars, 180°C and 250 °C. The residence time was 4 h with a heating rate of 8 °C/min. It took 15–25 min to reach the desired temperature. After carbonization, the mixture was allowed to cool to room temperature and then filtered. The solid material was washed until clear water was obtained. Hydrochar was then dried in an oven at 105°C for 24 h, ground and sieved through a mesh of 0.5 mm to homogenize the size of the hydrochar particles. The hydrochars derived from CP and CH at 180°C were designated as CP180 and CH180, while those produced at 250°C were labelled CP250 and CH250.To produce biochars, coffee pulp hydrochars were pelletized and then pyrolysed at two temperatures, 600 and 800°C, for 30 s (fast pyrolysis), resulting in biochars labelled as CP180–600 and CP250–600, as well as CP180–800 and CP250–800. The same pyrolysis conditions were applied to coffee husks, producing CH600 and CH800. The biochar particles were also harmonized at 0.5 mm. In total, four hydrochars and six biochars were produced.

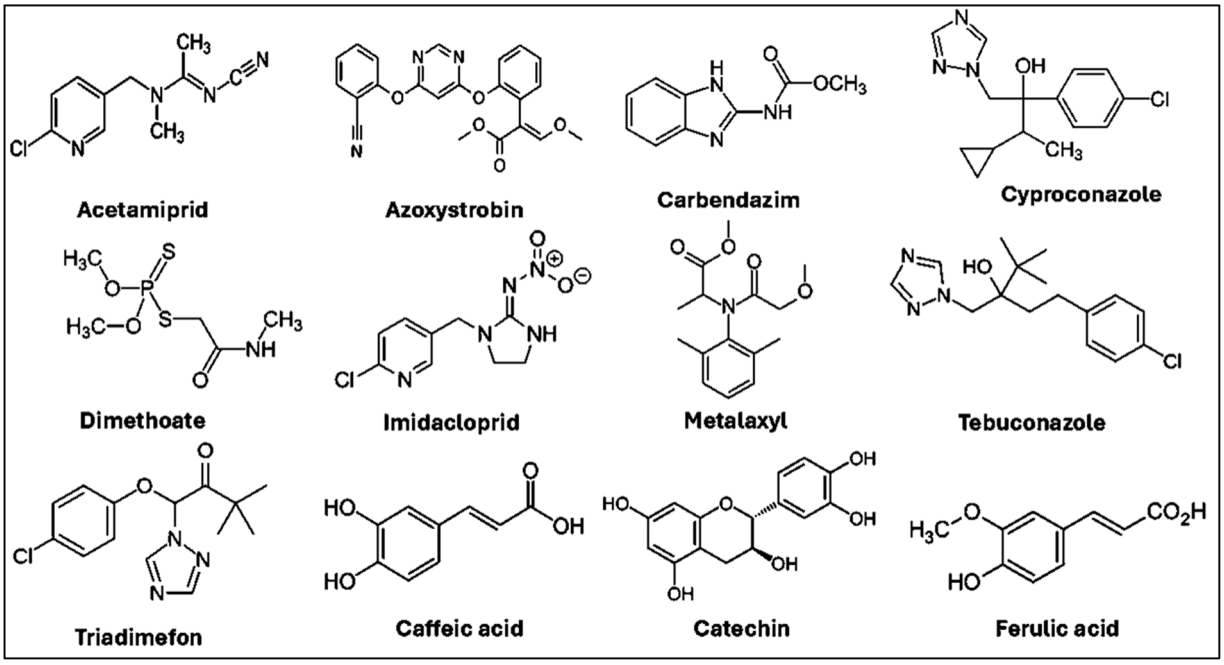

Fig. 1. Molecular structure of polyphenols; caffeic acid, catechin and ferulic acid, and the pesticides; acetamiprid, azoxystrobin, carbendazim, cyproconazole, dimethoate, metalaxyl, tebuconazole and triadimefon that were selected for this study.

2.3. Surface characterisation of hydrochars and biochars

Diffuse Reflectance Infrared Fourier Transform Spectroscopy (DRIFTS) and Raman spectroscopy were conducted to analyse the chemical functional groups on the biochar and hydrochar surfaces. For the DRIFTS analysis, 10 mg of the sample was mixed with 390 mg of KBr (Merck, Darmstadt, Germany), which is used for FTIR spectroscopy, and the mixture was manually ground in an agate mortar. The spectra were recorded under vacuum conditions specific to diffuse reflectance, utilising a Bruker IFS 66 v/S FTIR spectrometer (Bruker Optik GmbH, Ettlingen, Germany). Data collection spanned from 400 to 4000 cm^{-1} with a resolution of 4 cm^{-1}. Raman spectroscopy was conducted with samples placed in glass vials, using a Bruker Bravo spectrometer across the full range of automatic settings. The spectra were trimmed to 300–1900 cm^{-1} for data processing, a normalisation vector was applied across the entire spectral range, and smoothing was performed using the Savitzky-Golay algorithm with 13 points. The procedures and analysis of the spectra adhered to those described in our previous publication (Mukarunyana et al., 2023).

X-ray photoelectron spectroscopy (XPS) was performed to determine the atomic percentages of chemical elements on the surface of the biochar and hydrochar samples. A clean spatula was used to press a powdered sample, forming a pellet on the sample holder. Spectra were obtained using a monochromatic source electron spectrometer (Kratos Axis Ultra DLD) operating at 120 W. The analyser passes energies of 160 eV for wide spectra and 20 eV for photoelectron lines, facilitating the acquisition of relevant data. The binding energy scale was calibrated against the aliphatic carbon (C1S line), set at 285 eV. The spectra were analyzed using Kratos software.

The Brunauer-Emmett-Teller (BET) method was used to determine and calculate the specific surface area, volume, and pore size of hydrochars and biochars. To this end, nitrogen gas adsorption-desorption was used.

2.4. pH determination

The pH of hydrochars and biochars was obtained by mixing a 1:10 ratio (mg/ml) of sample and MilliQ water. The solution was shaken for 4 h at 34 rpm at room temperature (21°C), allowing it to equilibrate. Subsequently, the mixture was centrifuged for 15 min at 3500 rpm. The pH of the supernatant was measured using a pH meter. The pH of CPWW was also taken.

2.5. LC-MS/MS analysis

The selected compounds for analysis in coffee processing wastewater (CPWW) samples collected in a washing station in Rwanda were quantified using ultra-high-performance Liquid Chromatography coupled with tandem Mass Spectrometry (UHPLC-MS/MS). The analysis was conducted using a Dionex UltiMate 3000 UHPLC system, which features two LC pumps (an Ultimate LPG 3400 SD quaternary pump and an HPG 3400RS binary UHPLC pump) in addition to an analytical column (Thermo Scientific Hypersil GoldAq3, 100 × 2.1 mm, 3 μm) and a precolumn (Hypersil GOLD, 10 × 2.1 mm, 3 μm), all connected to a TSQ Quantiva triple quadrupole mass spectrometer (Thermo Scientific). A heated-electrospray ionisation (HESI) source was employed, operating in either positive or negative ion mode. Chromeleon Xpress (Thermo Scientific) was used to manage the UHPLC system. The chromatographic separation process involved a gradient of Milli-Q water and methanol (LiChrosolv, Merck, Darmstadt, Germany). The mobile phase comprised a gradient of 0.1 % formic acid in Milli-Q water and 0.1 % formic acid in methanol. The resolution for both quadrupole instruments was set to 0.7 full width at half maximum height. The spray voltage was fixed at 3500 V, with sheath gas at 40 arbitrary units, sweep gas at zero arbitrary units, ion transfer tube temperature at 350 °C, and vaporizer temperature at 338 °C. Two MS/MS transitions were monitored for each analyte: one for quantification and the other for qualification. Details regarding MS/MS transitions, associated collision energies, relevant internal standards, and retention times for each analyte are outlined in Table S2 (supplementary material). Peak identification was achieved by comparing components from the samples with those of internal standards using Xcalibur™ 4.3 software (Thermo Fisher Scientific). A seven-point calibration curve ranging from 1 to 100 mg/L was employed to assess linearity and perform quantification.

2.6. Adsorption experiments

Before the adsorption experiments, CPWW was analysed using the LC-MS/MS method, as explained in Section 2.5, to check the concentrations of the selected 12 compounds. After checking concentrations in CPWW, solutions containing all compounds were prepared for adsorption experiments. Specifically, six millilitres of a stock solution at one mg/ml were spiked into 144 ml of CPWW to create a 150 ml solution with a concentration of 40 mg/L in a 250 ml Erlenmeyer flask. Experiments were conducted at 22 °C in triplicate, utilising 25 mg (± 2.5 mg) of hydrochar or biochar and 5 ml (± 0.01 ml) of CPWW in 15 ml plastic (Falcon) tubes. The hydrochar or biochar was weighed, and the CPW sample was introduced into the tube. The mixture was shaken for 1 h at room temperature (22∘C) at 34 rpm. The experiments concluded with the centrifugation of the samples for 15 min at 4000 rpm. The supernatant was transferred to a vial, into which internal standards were incorporated. The samples were analysed within 24 h. Triplicate blank samples (Milli-Q water without biochar) were also prepared and assessed. The adsorption of analytes onto the tube walls was examined through a triplicate test with tubes (1 mg/L of each analyte added in Milli-Q water, without biochar). Interactions between analytes were also tested using CPWW spiked with analytes (without adsorbent). The CPWW used to determine removal rates in the experiments was similarly agitated for 1 h in test tubes (without adsorbent). The removal efficiency (R%) was calculated using Equation (1).

$R\% = \frac{(C_o - C_f)}{C_o} \times 100$ (1) C_o and C_f (mg/L) represent the initial and final concentrations. From these adsorption experiments, one

adsorbent, CP250, was selected based on its removal efficiency in order to evaluate the impact of time on the adsorption process and to determine its adsorption capacity. Five solutions with concentrations of 10, 30, 50, 75, and 100 mg/L were prepared, and 75 mg of adsorbent was added to 5 ml of each solution. Aliquots were taken after 5, 10, 20, 30, 60, 90, and 120 min. Additional 10 mg/L solutions were prepared using MilliQ water to evaluate changes in the surface chemical functional groups of CP250 before and after adsorption. The analytes adsorbed per unit weight of adsorbent (adsorption capacity) at equilibrium, q_e (mg/g), and at a given time, t, during the adsorption process, q_t (mg/g), were obtained using Eq. (2) and Eq. (3).

$$q_e = \frac{(C_o - C_e) \times V}{M} \tag{2}$$

$$q_t = \frac{(C_o - C_t) \times V}{M} \tag{3}$$

C_o (mg/L), C_e (mg/L) and C_t (mg/L) are the initial, equilibrium and final concentrations, respectively. V(L) is the volume of solution, and M (g) is the weight of the adsorbent.

2.7. Adsorption models

Various adsorption models were utilised to determine adsorption characteristics. This study employed the Langmuir, Freundlich, and Temkin isothermal adsorption models and pseudo-first-order and pseudo-second-order kinetic models.

The Langmuir isotherm model describes the process of monolayer adsorption at uniform sites on the surface of a solid adsorbent. Essentially, the Langmuir isotherm is characterised by a consistent approach to maximum adsorption, signifying the complete coverage of the solid's surface by a single adsorption layer (Langmuir, 1917; Mansoori et al., 2022). The Langmuir model parameters were calculated using Eq. (4).

$$q_e = \frac{K_L q_{\max} Ce}{1 + K_L Ce} \tag{4}$$

where Ce (mg/L) denotes the concentrations at equilibrium, q_e and q_{max} (mg/g) represent the adsorption capacity at equilibrium and the maximum amount of analytes adsorbed per unit weight of adsorbent, respectively. K_L (L/mg) is the Langmuir constant, which pertains to the attraction between the adsorbate and adsorbent. The graph was plotted as C_e/q_e against C_e, with q_{max} and K_L derived from the plot.

The Freundlich isotherm model, expressed as Eq. (5), is commonly used to describe the adsorption characteristics of heterogeneous surfaces (Chiban et al., 2011; Lima et al., 2015).

$$q_e = K_F C_e^{\,1/n} \tag{5}$$

Where q_e (mg/g) is the adsorption capacity at equilibrium, and C_e (mg/L) represents the concentration at equilibrium. K_F [(mg/g)(L/mg)] is the Freundlich constant, while n is a constant related to the adsorbent surface heterogeneity and the intensity of adsorption. K_F and n were determined using the slope and intercept of the graph of log q_e versus log C_e.

The Temkin isotherm model expresses a linear relationship between adsorption energy and surface coverage. It includes elements that directly reflect the interactions between adsorbents and adsorbates (Dada, A.O et al., 2012). Eq. (6) represents the model by disregarding the very low and very high concentration values.

$$q_e = B_T \ln(A_T C_e) \tag{6}$$

q_e is the adsorption capacity at equilibrium, A_T is the Temkin constant related to binding energy, B_T is the Temkin constant related to the heat of adsorption and C_e is the concentration at equilibrium.

Equations (7) and (8) describe the pseudo-first-order (PFO) and pseudo-second-order (PSO) kinetic models, respectively.

$$Pseudo - first\ order : q_t = q_e(1 - e^{-k_1 t}) \tag{7}$$

$$Pseudo - secondorder : q_t = \frac{{q_e}^2 k_2 t}{1 + k_2 q_e t} \tag{8}$$

where t represents time in minutes, k_1 and k_2 are the first- and second-order kinetic adsorption constants, and q_t and q_e denote the adsorption capacity at time t and at equilibrium, respectively.

The model performance was evaluated using the coefficient of determination, R^2, in terms of best fit.

Finally, the intraparticle diffusion model was applied to evaluate the contribution of intraparticle mass transfer to the overall adsorption kinetics. The model is described by the Weber-Morris equation (9)

$q_t = K_{id} t^{1/2} + C$ (9) The model describes the relationship between adsorbate uptake and the square root of contact time, where q_t(mg/g) is the amount of solute adsorbed at time t, K_{id}(mg.g^{-1}min$^{-1/2}$) is the intraparticle diffusion rate constant, and C(mg.g^{-1}) is the intercept related to the boundary-layer effect. For each experimental concentration, q_t values were plotted against $t^{1/2}$. The parameters and C were obtained from the slope and intercept of the linear regression, respectively. The goodness of fit was assessed using

the coefficient of determination (R^2).

3. Results and discussions

3.1. Surface characterisation of biochars and hydrochars

Data from DRIFTS show that nearly all bands ranging from 500 to 4000 cm^{-1} decreased as the carbonisation temperature increased, resulting in a wide range of vibration peaks in hydrochars compared to those in biochars, since HTC occurred at 180 and 250 °C, while pyrolysis took place at 600 and 800 °C. A broad band between 3270 and 3520 cm^{-1} was detected in hydrochars but not in biochars, corresponding to the O-H stretching vibration, which might originate from hydroxyl groups of alcohols, carboxylic acids, or phenolic compounds. Also, in hydrochars and biochars, the sharp peaks between 2800 and 3000 cm^{-1} were assigned to symmetric and asymmetric aliphatic carbon (C-H) stretching in methyl (CH_3) and methylene (CH_2) groups. Compared to hydrochars, the peak intensities of O-H, CH_3 and CH_2 chemical functional groups noticeably decreased in biochars produced at 600 °C and completely disappeared in biochars produced at 800°C, as shown in Fig. 2(A) and (B). With the increase in carbonisation temperature, volatile compounds are reduced due to dehydration, decarboxylation and the breakdown of nonpolar aliphatic components (Fu et al., 2019; Janu et al., 2021). Furthermore, when carbonisation temperatures reach 600 °C, nearly all aliphatic functional groups in the biochar are eliminated; these aliphatic structures tend to transform into aromatic ones, leading to an increased presence of phenolic and ether groups (Fu et al., 2019; Janu et al., 2021; Zhang et al., 2020). Peaks at 1740 cm^{-1} in hydrochars and biochars were attributed to stretching vibrations from unconjugated and conjugated carbonyl groups (C═O) in aldehydes or ketones (Sathish and Saraswat, 2025). Bands observed at 1500 and 1597 cm^{-1} suggested aromatic carbon rings, -C═C- (Fu et al., 2019), and those observed at 889 and 873 cm^{-1} indicated the aromatic bending vibration and stretching of aliphatic C–H. These peaks were very weak in biochars produced at 800 °C compared to those produced at 600 °C. At higher temperatures (> 600 °C), numerous C═C bonds break due to the ample energy available; as a result, extensive carbonisation occurs, resulting in the formation of graphite-like structures within the biochar that display less pronounced peaks (Elnour et al., 2019; Wan et al., 2024). Peaks at 1150, 1240, 1370, and 1460 cm^{-1} in hydrochars and biochars were associated with -C-O-C-, -C-O or C-N, -C-H, and bending C-H vibrations, respectively. Weaker peaks between 950 and 1100 cm^{-1} in hydrochars and biochars could be linked to sugar rings involved in carbohydrate motions, including those in polysaccharides. The same functional groups were identified in charcoal derived from spent coffee grounds, which were prepared and used as an adsorbent (Milanković et al., 2024; Romero et al., 2025). The findings from DRIFTS and Raman analyses suggest that, with increasing carbonisation temperature, the organic matter was consistently decomposed, altering the structural composition of the organic material and demonstrating that the breakdown became increasingly thorough and complete (Wan et al., 2024; Zhu et al., 2023).

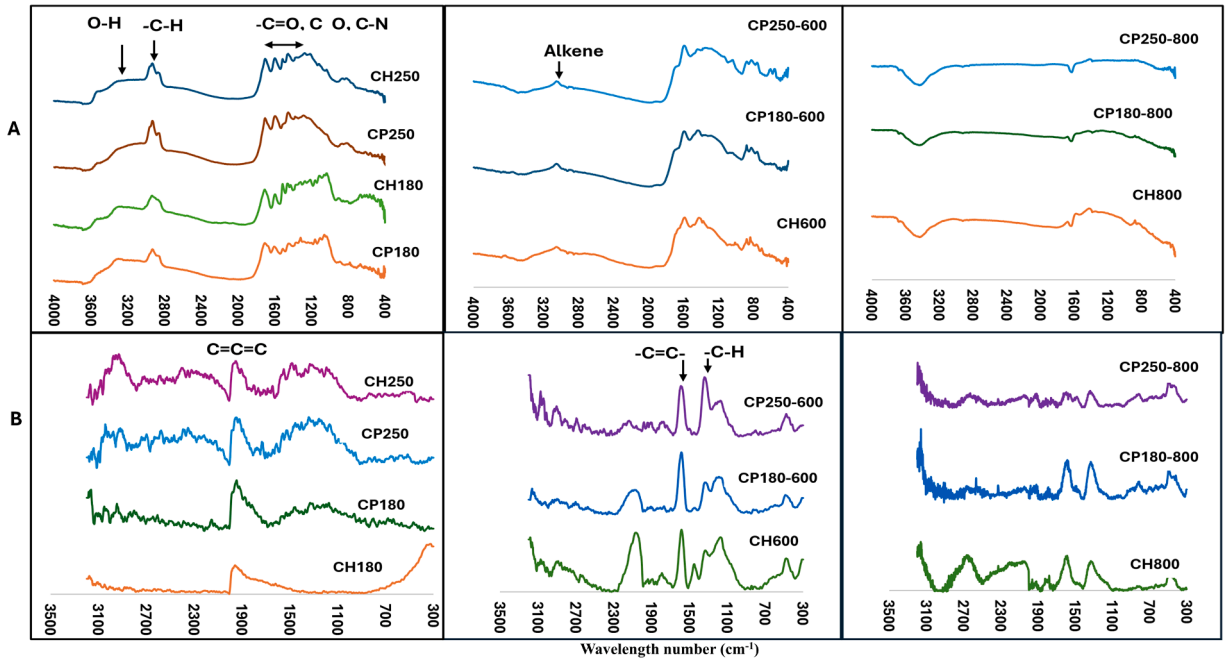

Fig. 2. Spectra from DRIFTS (A) and Raman (B). (A) indicates the main chemical functional groups, O-H, C-H, C═O, C-O and C-N on the surface of hydrochars and biochars produced from coffee pulp at 180 and 250°C (CP180, CP250, CH180, CH250) as well as biochars produced at 600 and 800°C from coffee pulp and husk (CP180–600, CP250–600, CP180–800, CP250–800, CH600 and CH800). (B) shows intensities of aliphatic, C-H and aromatic, C═Cor C═C═C groups.

The X-ray spectroscopy data shown in Table 1 revealed differences in the elemental composition of hydrochar and biochar surfaces. The carbon (C) content ranged from 72.7 % to 84.5 %, being lower in hydrochars produced at 180 °C (72.7 % and 77.8 % in CH180 and CP180, respectively) than in biochars (79.4–84.5 %). Conversely, the oxygen (O) percentage varied from 26.2 % to 7.42 %, with 26.2 % and 20.8 % in CH180 and CP180, and 17.6 % and 15.6 % in CH250 and CP250, respectively. The lower O values were observed in biochars produced at 600 °C (12.2–8.35 %) and at 800 °C (7.74–7.42 %). These findings indicate that C content increases with higher carbonisation temperatures, probably due to a greater degree of carbonisation at elevated temperatures. The reduction in oxygen (O) content with increasing pyrolysis temperature may be attributed to the volatility of organic materials and/or the breakdown of weaker oxygen and hydrogen bonds, which are found in hemicellulose, cellulose, and lignin, during high-temperature pyrolysis (Handiso et al., 2024; Romero et al., 2025; Toczydlowski et al., 2023). Consequently, the atomic ratio O/C, used as an indicator of polarity, decreased as the carbonisation temperatures increased (De Jager et al., 2022; Handiso et al., 2024). The decline in the O/C ratio at higher pyrolysis temperatures indicates the reduction of polar content, which can enhance the surface hydrophobicity of biochar (Handiso et al., 2024; Vijayaraghavan and Balasubramanian, 2021).

The elemental analysis also revealed that some minerals were only present in biochars, such as K, which ranged from 4.12 % to 7.63 %, and Ca, spanning from 0.67 % to 3.14 %. It has been reported that the composition of essential elements increases with pyrolysis temperature, mainly due to the concentration of these elements in biochar samples at higher temperatures (Al-Wabel et al., 2013; Tang et al., 2019; Xu et al., 2021), 600°C and 800°C in the present study. This increase in alkaline elements could be responsible for the slight rise in pH observed in this study, as detailed in Table S3 of pH in the supplementary materials.

The findings from the BET analysis showed that biochars had higher specific surface areas (ranging from 21.2 to 33.7 m^2/g) compared to hydrochars (which ranged from 4.70 to 15.7 m^2/g), indicating that specific surface areas increase with higher carbonisation temperatures (Mobarak et al., 2024).

The increase in surface area in biochars results from chemical reactions caused by the carbonisation temperature, which removes phenolic and hydroxyl groups attached to aromatic structures, as well as aromatic carbonyls and aliphatic alkyl and ester carbonyl groups that cover the aromatic core (Oginni and Singh, 2020). During carbonisation, the loss of volatile components from the biomass creates pores (Prahas et al., 2008).

3.2. Removal efficiency of hydrochars and biochars

Fig. 3 illustrates the removal efficiency (R%) of hydrochars (CP 180, CH 180, CP 250, and CH 250) and biochars (CP 180–600; CP 250–600, CH 600, CP 180–800; CP 250–800, and CH 800) for the polyphenols and pesticides studied. Hydrochars strongly adsorbed CAF, CAT and FER, probably due to the linkage between hydroxyl groups of these polyphenolic compounds and those on the hydrochar surface via hydrogen bonds (Mounia et al., 2009). The same reasoning applies to CAR. Conversely, AZO, CYP, and MET (fungicides) were better adsorbed by biochars. DIM (organophosphate insecticide) and IMD (neonicotinoid insecticide) preferred hydrochars, while biochars effectively adsorbed TEB and TRI (fungicides). Both hydrochars and biochars adsorbed ACE (neonicotinoid insecticide) and TEB (fungicide) almost equally. Another key factor is the acid dissociation constant, pKa, which indicates how likely an acid is to dissociate into ions in water. A low pKa means an acid dissociates easily in water (Pagni, 2006). Since the solutions were prepared using CPWW, which is acidic (pH = 3.5), CAF, FEA, and CAT were in a non-ionised state; these compounds showed high R%, suggesting that the lack of electrostatic interactions among molecules may have enhanced their adsorption (Solomakou et al., 2023). Pesticides such as AZO, CYP, MET, TEB, and TRI, which were well adsorbed by biochars, generally have high molecular weights (279–403.4 g/mol) and octanol-water partition coefficients, K_{OW} (log K_{OW} ranging from 2.19 to 3.7), compared to other selected compounds. A high K_{OW} indicates that these pesticides are hydrophobic. Consequently, they are likely to be adsorbed to biochars through hydrophobic interactions, as the produced biochars had low O/C ratios (<0.2), indicating high surface hydrophobicity (Bakshi et al., 2020). As shown in various studies on the adsorption of different pesticides onto biochars produced from various feedstocks, pesticide adsorption might also involve π- π-electron interactions, especially for aromatic pesticides. Aromatic rings result in delocalised electrons, creating electron-rich and electron-deficient regions (Zhang et al., 2020). When aromatic pesticides approach the aromatic rings on the biochar surface, π- π stacking interactions can occur (Celis et al., 2000; Dong et al., 2024; Mosquera-Vivas et al.,

Table 1
Atomic percentages of elements on the surface of biochars and hydrochars from XPS, and their specific surface area S_{BET} (m^2/g) and pore size P_{BET} (nm) from BET analysis using N_2 gas.

	C	O	N	K	Ca	Cl	O/C	S_{BET} (m^2/g)	P_{BET} (nm)
CP180	77.8	20.8	1.40	-	-	-	0.20	5.80	2.52
CH180	72.7	26.2	1.10	-	-	-	0.27	4.70	2.11
CH250	80.8	17.6	1.60	-	-	-	0.16	12.9	2.33
CP250	82.5	15.6	1.90	-	-	-	0.14	15.7	3.12
CH600	79.4	12.2	1.16	6.22	1.02	-	0.12	21.4	2.64
CP180–600	83.5	9.62	1.83	4.12	0.93	-	0.09	21.2	3.23
CP250–600	84.5	8.35	1.69	4.79	0.67	-	0.07	30.9	3.71
CP180–800	81.3	7.74	1.64	7.17	2.15	0.64	0.07	27.2	2.62
CP250–800	80.2	7.62	1.41	7.63	3.14	0.38	0.07	25.6	2.27
CH800	82.1	7.42	1.35	7.38	1.75	0.48	0.07	33.7	3.35

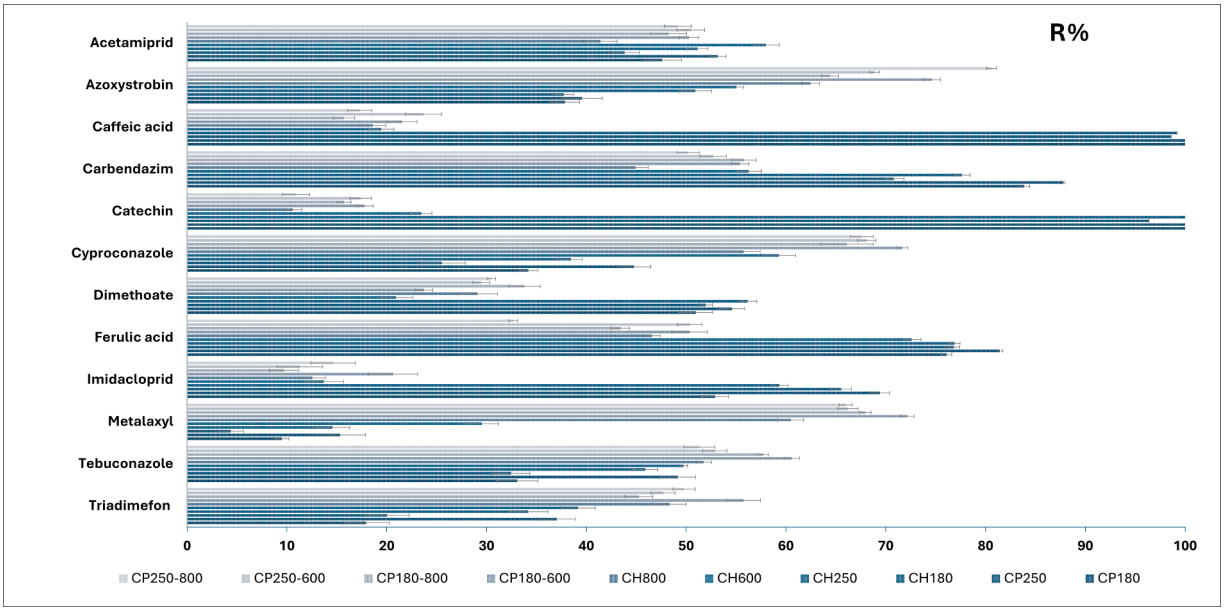

Fig. 3. Removal efficiencies in percentage (R%) of hydrochars produced from coffee pulp and husk at 180 and 250 °C (CP180, CP250, CH180, CH250), and biochars produced at 600 and 800 °C from coffee pulp and husk (CH600, CP180–600, CP250–600, CP180–800, CP250–800 and CH800) for Acetamiprid, Azoxystrobin, Caffeic acid, Carbendazim, Cyproconazole, Dimethoate, Ferulic acid, Imidacloprid, Metalaxyl, Tebuconazole and Triadimefon considering 5 ml of 40 mg/L, 25 mg of adsorbents and a contact time of 60 min.

2018). This non-covalent force involves attractive interactions between parallel or nearly parallel electron-rich systems, helping to stabilise pesticide molecules on the biochar surface (Dong et al., 2024). Furthermore, results from CP250 DRIFTS spectra before and after adsorption of all analytes showed that peak intensities decreased in the 620–671 cm^{-1} region, which is characterized by aromatic functional groups (Dong et al., 2024). This indicates their involvement in the adsorption process, as all analytes contain aromatic rings. Furthermore, there was a reduction in spectral intensities at 1033 and 1120 cm-1, at 2870–2930 cm-1, and 3200–3550 cm-1, regions characteristic of C-O or C-O-C in ether, ester, or phenolic groups, C-H aliphatic, and O-H groups, respectively (Mounia et al., 2009), as

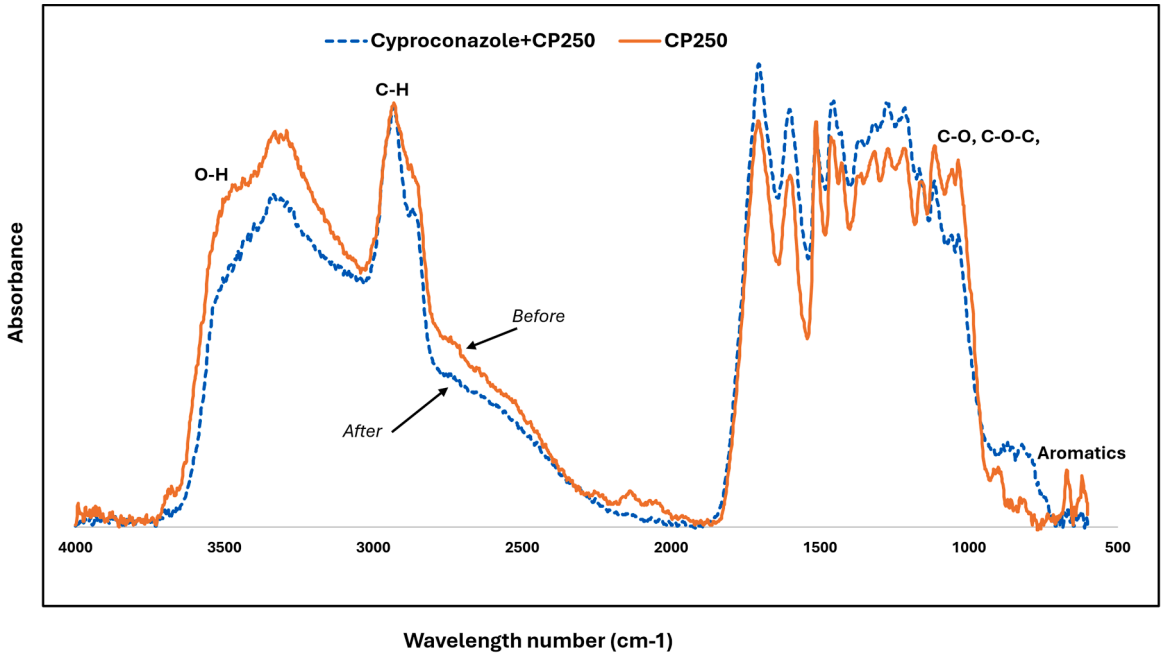

Fig. 4. DRIFTS spectra of hydrochar derived from coffee pulp at 250°C (CP250) before and after adsorption of cyproconazole. Raw data and graphs for all pesticides and polyphenols are presented in Table S5, in the supplementary material.

shown in Fig. 4 taken as an example of DRIFTS graphs produced with CP250 before and after adsorption. This decrease may suggest that these functional groups participate in adsorption via hydrogen bonding, with oxygen acting as the acceptor, and/or dipole-dipole interactions (Solomakou et al., 2023). Raw data from adsorption experiments are provided in Table S4 of the supplementary materials, and data from CP250 DRIFTS before and after adsorption are presented in Table S5 of the supplementary materials.

3.3. Adsorption isotherms

The data from batch adsorption experiments were analyzed using isotherm models. Studying adsorption isotherm models is essential for understanding equilibrium data and gaining insights into the adsorption processes at the active surface sites of the adsorbent. In this study, the non-linear representations of three equilibrium isotherm models, Langmuir, Freundlich, and Temkin, were utilised on the experimental data for ACE, AZO, CAF, CRB, and CYP, DIM, CAT, IMD, MET, TEB, and TRI adsorption on CP250 absorbent. The adsorption isotherms and the fitting parameters for the Langmuir, Freundlich and Temkin models are presented in Table 2 and Figure S1 in the supplementary material. The coefficient of determination (R^2) indicated that the Freundlich model could provide better adsorption descriptions of the studied compounds than the Langmuir model. The R^2 values for the Freundlich model ranged from 0.865 to 1.000. Since the Freundlich model fitted the experimental data well (high R^2 values), it was suggested that the adsorption of ACE, AZX, CRB, CAT, CYP, FEA, IMD, MET, TEB, and TRI onto CP250 hydrochar took place through multilayer adsorption on the heterogeneous surface of CP250, which therefore contained various active sites. These findings align with those of previous studies on pesticide adsorption onto different adsorbents (Chiban et al., 2011; Lima et al., 2015). Furthermore, Srikhaow et al. (2022) reported that ACE and IMD experimental data were described by the Freundlich model when investigating the adsorption of these pesticides on eucalyptus wood biochar; Fruehwirth et al., (2020) argued that the same isotherm model fitted atrazine pesticide on three biochars derived from wood industry byproducts with R^2= 0.998, 0.987, and 0.892. The same model explained the adsorption of multiple pesticides on coconut shell modified biochar (Cao et al., 2023; Fruehwirth et al., 2020; Srikhaow et al., 2022). Although the R^2 values for the Freundlich model were higher than those of the Langmuir model in this study, the adsorption of three compounds, ACE, CRB, and IMD, could also be explained by the Langmuir model with a low contribution. R^2 ranged from 0.774 to 0.868 for the Langmuir model. These findings demonstrate the complexity of the adsorption mechanisms of organic compounds (Elliott and Huang, 1979). Adsorption of DIM on CP250 was well described by the Temkin model, with $R^2 = 0.993$, whereas both the Langmuir and the Freundlich models had low R^2 values, of 0.687 and 0.633, respectively.

Both the Langmuir and Freundlich models had relatively low and almost exactly equal values of R^2 for DIM, 0.685 and 0.633, respectively. However, the Temkin model provided the best fit for that pesticide with $R^2 = 0.993$, indicating that the heat of adsorption for DIM molecules in the layer decreases linearly as coverage increases, due to interactions between the adsorbent and adsorbate. This predictability in the reduction of heat of adsorption enhances understanding of the process. Furthermore, it shows that the adsorption process involves a consistent distribution of binding energies, reaching a maximum binding energy (Hamdaoui and Naffrechoux, 2007). Both Temkin and Freundlich also gave a better fit for the experimental data for AZO, MET, and TRI, as indicated by the R^2 values of those two models shown in Table 2. Experimental data for caffeic acid were not analysed using the considered isotherm models because qe and qt were zero, demonstrating that the concentrations used in this study were low and all caffeic acid molecules had been adsorbed on CP250. Furthermore, caffeic acid has a lower molecular mass (180.2 g/mol) than the other compounds considered (which vary between 191.2 and 403.4 g/mol); this may favour the pore-filling mechanism on the adsorbent (Kalinke et al., 2020), along with hydrogen bonding interactions from the hydroxyl groups of caffeic acid and those of CP250 (Solomakou et al., 2023). Langmuir parameters indicated that the maximum adsorption capacities, q_{max}, of carbendazim and ferulic acids, both with low molecular masses (191.2 and 194.2 g/mol), were high compared to those of other compounds (5.33 ± 1.28 and 7.83 ± 4.24 mg/g), also suggesting the involvement of pore filling interactions on CP250 in addition to other adsorption mechanisms mentioned above. Literature does not present many published articles on adsorption by hydrochars of the compounds considered in this study. The available data relate to their adsorption by biochars in a distilled water matrix, rather than in a more complex matrix as was the case here. This may explain why the qmax values obtained were relatively low. The chemical complexity, competing natural organics, and inherent organic load of coffee wastewater are likely to cause a marked reduction in the q_{max} of CP250 for externally introduced

Table 2
Parameters of the Langmuir, Freundlich, and Temkin isotherms for the adsorption of the chemicals under study on the CP250 adsorbent.

	Langmuir			Freundlich			Temkin		
	q_{max} (mg/g)	K_L(L/mg)	R^2	K_F(mg/g)(L/mg)	n	R^2	B_T	A_T	R^2
Acetamiprid	3.06	0.06	0.77	0.53	2.63	0.96	1.00	1.00	-
Azoxystrobin	0.77	-	-	0.51	3.85	0.87	0.31	2.20	0.94
Carbendazim	5.33	0.15	0.88	1.21	2.56	0.97	1.00	1.00	0.20
Catechin	3.87	0.33	-	1.96	5.56	1.00	0.64	9.18	0.95
Cyproconazole	0.19	-	-	0.53	2.94	0.95	0.31	0.06	0.04
Dimethoate	2.37	5.29	0.68	1.65	9.09	0.63	0.22	1.91	0.99
Ferulic acid	7.83	1.69	-	5.00	1.82	0.99	1.20	4.45	0.90
Imidacloprid	3.23	0.32	0.88	1.23	4.00	0.99	1.00	1.00	0.34
Metalaxyl	1.55	-	-	0.24	2.22	0.95	0.43	0.48	0.97
Tebuconazole	0.45	-	-	0.79	4.76	0.87	1.00	1.00	-
Triadimefon	1.69	-	-	0.30	2.33	0.96	0.47	0.55	0.97

pesticides or polyphenolic pollutants compared to values obtained under simplified laboratory conditions. Table 3 shows reported q_{max} values for various biochar and hydrochar.

3.4. Adsorption kinetics

The results from adsorption kinetics experiments showed that the adsorption of all selected compounds generally occurred rapidly during the first 20 min and gradually approached the limiting adsorption after 60 min, as shown in Figure S2 in the supplementary materials. Experimental data was described using PFO, PSO and intraparticle diffusion models. The PFO model is a clear and straightforward tool that typically presumes a direct relationship between the adsorption capacity and the difference between the concentration at a specific contact time and the equilibrium concentration. In this model, the rate of adsorbent site occupation is directly governed by the quantity of unoccupied sites (Khamwichit et al., 2022; Liu et al., 2019). The PSO is frequently linked to chemisorption, which involves stronger chemical bonds and can effectively represent the overall adsorption process, particularly when chemical interactions play a role (Tran et al., 2020). Comparing the values of R^2 of those models, as shown in Table S6, it was found that both PFO and PSO provided a good fit to the experimental data, apart from caffeic acid, catechin and imidacloprid at 10 mg/L, where the PSO model described the experimental results (R^2 for PSO: 1, 1, and 0.888, respectively). This indicates that chemisorption strongly dominated the adsorption process, suggesting that the adsorption process of selected compounds was complex and probably involved diverse mechanisms. Although both the PFO and PSO models fitted the remaining adsorption data, the PSO model described the data well at high concentrations (75 and 100 mg/L), as indicated by the R^2 values. Also, the intraparticle diffusion plots for all studied analytes exhibited a clear multi-linear trend, indicating that the adsorption process occurs through multiple sequential kinetic stages rather than being controlled solely by intraparticle diffusion (Tong et al., 2019). For all initial concentrations, the first linear segment displayed a steep slope, corresponding to rapid adsorption onto the external surface of CP250. This phase is governed primarily by boundary-layer (film) diffusion, during which analyte molecules migrate from the solution to the sorbent surface (Weber Jr & Morris, 1963). Following this initial stage, the plots transition into a second region with a lower slope, indicating the slower diffusion of molecules into the internal pore network of the CP250 matrix. According to the Weber–Morris intraparticle diffusion model, a straight line passing through the origin (0,0) indicated that intraparticle diffusion is the sole rate-limiting step; however, none of the linear portions in the present study extrapolated to the origin, as shown by Figure S3 in the supplementary materials. Kid and C values are presented in Table S6. This deviation confirms that intraparticle diffusion is not the only rate-controlling mechanism and that both film diffusion and pore diffusion contribute to the overall adsorption kinetics (Ho and McKay, 1999; Weber Jr & Morris, 1963). The multi-linearity is more pronounced at higher initial concentrations (75–100 mg/L), suggesting that an increased concentration gradient enhances the driving force for mass transfer. At extended contact times (from 30 min), the diffusion curves approach a plateau, indicating that adsorption equilibrium has been reached and that the available active sites on the CP250 surface and within its

Table 3
The maximum adsorption capacities (q_{max}) determined in this study and those in the literature for biochars and hydrochars adsorbing the selected compounds (Anićijević et al., 2023; Ayeb et al., 2024; Chen et al., 2024; Dávila-Guzman et al., 2012; Duran et al., 2024; Gomes et al., 2025; Lee et al., 2021; Liu et al., 2018; Prelac et al., 2023; Soetaredjo et al., 2013; Srikhaow et al., 2023; Xiang et al., 2023).

Compound	Adsorbent	Q_{max} (mg /g)	Remarks	Source
Azoxystrobin	Hydrochar from coffee pulp	0.77	CPWW[a]	This study
	Activated biochar *Molinga Oleifera*	1.66–11.2	DW[b]	Gomes et al., (2025)
Acetamiprid	Hydrochar from coffee pulp	3.06	CPWW[a]	This study
	Eucalyptus-wood biochar	4.87	DW[b]	Srikhaow et al., (2022)
	Optimized vine-pruning hydrochar	5.02	DW[b]	Duran et al., (2024)
Caffeic acid	Biochar from grapevine residues	5.73	DW[b]	Prelac et al., (2023)
Carbendazim	Hydrochar from coffee pulp	5.33	CPWW[a]	This study
	Peanut shell biochar	17.7	DW[b]	Lee et al., (2021)
Catechin	Hydrochar from coffee pulp	3.87	CPWW[a]	This study
	Cellulose powder	2.70–2.82	DW[b]	Liu et al., (2018)
	Activated carbon	73.6	DW[b]	Soetaredjo et al., (2013)
Cyproconazole	Hydrochar from coffee pulp	0.19	CPWW[a]	This study
Dimethoate	Hydrochar from coffee pulp	2.37	CPWW[a]	This study
	Viscose fibre-derived biochar	< 15	DW[b]	Anićijević et al., (2023)
	Agricultural-waste biochars	3.57	DW[b]	Ayeb et al., (2024)
Ferulic acid	Hydrochar from coffee pulp	7.83	CPWW[a]	This study
	Magnetic lignin-based biochar	20.5	DW[b]	Xiang et al., (2023)
	Activated carbon from pine	127.3	DW[b]	Dávila et al. (2012)
Imidacloprid	Hydrochar from coffee pulp	3.23	CPWW[a]	This study
	Eucalyptus-wood biochar	14.75	DW[b]	Srikhaow et al., (2022)
Metalaxyl	Hydrochar from coffee pulp	1.55	CPWW[a]	This study
	Pristine vine pruning biochar	1.73	DW[b]	Duran et al., (2024)
Tebuconazole	Hydrochar from coffee pulp	0.45	CPWW[a]	This study
	Peanut shell biochar	20.5	DW[b]	Lee et al., (2021)
Triadimefon	Hydrochar from coffee pulp	1.69	CPWW[a]	This study
	Biochar-based MgO_2 composite	8.89	DW[b]	Chen et al., (2024)

[a] Coffee processing wastewater (CPWW), [b] Distilled water (DW)

pore structure have become progressively saturated. Overall, the kinetic behaviour observed was consistent with adsorption mechanisms reported for other organic contaminants on biochar and carbonaceous adsorbents, where a rapid surface-controlled phase is followed by slower intraparticle diffusion due to the heterogeneous pore structure of the sorbent (Ebelegi et al., 2020; Hwang et al., 2015; Tong et al., 2019; Wu et al., 2009).

3.5. Novelty of this study and implementation opportunities

The production of biochar and hydrochar from coffee processing by-products offers a promising and largely unexplored opportunity for sustainable wastewater management in coffee-producing developing countries such as Rwanda. While coffee husks and pulp contain abundant lignocellulosic compounds, they remain underutilized and can contribute to environmental degradation when left to decompose. At the same time, coffee washing stations produce large volumes of highly polluted wastewater rich in organic load, phenolic compounds, and caffeine, yet affordable and decentralized treatment solutions are scarce. This study introduced a novel circular bioresource approach by converting coffee waste (husk and pulp) into biochar and hydrochar through pyrolysis and hydrothermal carbonization respectively, and subsequently applying these locally derived adsorbents to treat wastewater generated during coffee processing. While existing research, typically addresses waste management, biochar and hydrochar production, or wastewater treatment independently, this study integrates these elements into a closed-loop system specifically tailored to the technical and socioeconomic realities of coffee cooperatives. Pyrolysis and hydrothermal carbonization not only align production methods with the moisture characteristics of each feedstock but also generate adsorbents with distinct surface chemistries that can target complex contaminants in coffee processing wastewater. This constitutes a significant contribution to both scientific literature and practical environmental management, offering a low-cost, decentralized, and context-appropriate technology that supports Rwanda's emerging circular economy agenda and enhances sustainability across the value chain. Production of biochar from solid waste through pyrolysis is a technology that is already commercially available worldwide (IBI, 2024), and this process generates a heat surplus when converting dry biomass into biochar. The management of spent filter material is an important issue to consider in further development. If stored in soil, biochar provides long-term carbon sequestration, bringing a climate benefit (Lehmann et al., 2021). However, the fate of the organic pollutants adsorbed to the biochar would require careful monitoring. Another option is to dry filters and use them as fuel, providing renewable energy, but again requiring careful consideration of organic pollutants.

4. Conclusion

In this study, four hydrochars and six biochars were produced from coffee pulps and husks using respectively HTC at 180 °C and 250°C and pyrolysis (N_2 gasification) at 600 °C and 800°C. Characterisation of these materials with DRIFTS showed that the surface of hydrochars were richer in OH and aliphatic groups than biochars. Additionally, XPS analysis confirmed these findings, demonstrating that the oxygen content was higher in hydrochars than in biochars. The results of the adsorption experiments demonstrated that hydrochars and biochars derived from coffee waste can remove selected polyphenols and pesticides from CPWW under the tested conditions. Generally, polyphenols were well adsorbed onto hydrochars, achieving R% varying between 76.1 % and 100 %, probably by involving hydrogen bonding interactions. Conversely, pesticides were predominantly adsorbed onto biochars, possibly through hydrophobic interactions. The adsorption isotherm analyses performed with CP250 showed that the Freundlich model best described the experimental data. In contrast, kinetic model analyses indicated that both PFO and PSO fitted the adsorption data, demonstrating the complexity of the adsorption mechanisms. The intraparticle diffusion model parameters also indicated that diffusion was not the only rate-limiting step in absorption. Further research could include a field study to investigate the loading of polyphenols and pesticides from coffee washing stations and optimise adsorption conditions to determine qmax for coffee-based biochars and hydrochars.

CRediT authorship contribution statement

Jerker Fick: Writing – review & editing, Visualization, Validation, Supervision, Resources, Project administration, Methodology, Funding acquisition, Data curation, Conceptualization. **Christoffer Boman:** Writing – review & editing, Visualization, Validation, Supervision, Resources, Project administration, Funding acquisition, Conceptualization. **Telesphore Kabera:** Writing – review & editing, Validation, Project administration, Conceptualization. **Cecilia Sundberg:** Writing – review & editing, Visualization, Supervision, Project administration, Funding acquisition, Conceptualization. **Brigitte Mukarunyana:** Writing – review & editing, Writing – original draft, Visualization, Validation, Software, Resources, Project administration, Methodology, Investigation, Formal analysis, Data curation, Conceptualization.

Declaration of Competing Interest

The authors declare the following financial interests/personal relationships which may be considered as potential competing interests: Brigitte Mukarunyana reports a relationship with Umeå University that includes: employment. Cecilia Sundberg reports a relationship with Swedish University of Agricultural Sciences that includes: employment. Telesphore Kabera reports a relationship with University of Rwanda that includes: employment. Christoffer Boman reports a relationship with Umeå University that includes: employment. Jerker Fick reports a relationship with Umeå University that includes: employment. If there are other authors, they declare that they have no known competing financial interests or personal relationships that could have appeared to influence the work reported in this paper.

Acknowledgements

The authors would like to thank the Swedish International Development Agency (SIDA), for financial support.

Appendix A. Supporting information

Supplementary data associated with this article can be found in the online version at doi:10.1016/j.eti.2025.104739.

Data availability

All raw data is included in the supplementary materials.

References

Alemayehu, Y.A., Asfaw, S.L., Terfie, T.A., 2021. Reusing coffee processing wastewater and human urine as a nutrient source: effect on cabbage cultivation. Waste Biomass.. Valoriz. 12 (11), 6165–6175. https://doi.org/10.1007/s12649-021-01451-9.

Alemayehu, Y.A., Asfaw, S.L., Tirfie, T.A., 2020. Management options for coffee processing wastewater. A review. J. Mater. Cycles Waste Manag. 22 (2), 454–469. https://doi.org/10.1007/s10163-019-00953-y.

Alves, R.C., Rodrigues, F., Nunes, M.A., Vinha, A.F., Oliveira, M.B.P., 2017. State of the art in coffee processing by-products. Handb. Coffee Process. Prod. 1–26. https://doi.org/10.1016/B978-0-12-811290-8.00001.

Al-Wabel, M.I., Al-Omran, A., El-Naggar, A.H., Nadeem, M., Usman, A.R., 2013. Pyrolysis temperature induced changes in characteristics and chemical composition of biochar produced from conocarpus wastes. Bioresour. Technol. 131, 374–379. https://doi.org/10.1016/j.biortech.2012.12.165.

Amare, G., Dobo, B., Haile, E., 2023. The effect of wet coffee processing plant effluent on physicochemical and bacteriological quality of receiving rivers used by local community: case of Aroresa District, Sidama, Ethiopia. Environ. Health Insights 17, 11786302231165186. https://doi.org/10.1177/11786302231165186.

Ameca, G.M., Cerrilla, M.E.O., Córdoba, P.Z., Cruz, A.D., Hernández, M.S., Haro, J.H., 2018. Chemical composition and antioxidant capacity of coffee pulp. Ciência e Agrotecnologia 42, 307–313. https://doi.org/10.1590/1413-70542018423000818.

Ameta, R., Chohadia, A.K., Jain, A., Punjabi, P.B., 2018. Fenton and photo-Fenton processes. Advanced Oxidation Processes for Waste Water Treatment. Elsevier, pp. 49–87. https://doi.org/10.1016/C2016-0-00384-4.

Anićijević, V., Tasić, T., Milanković, V., Breitenbach, S., Unterweger, C., Fürst, C., Bajuk-Bogdanović, D., Pašti, I.A., Lazarević-Pašti, T., 2023. How well do our adsorbents actually perform?—The case of dimethoate removal using viscose fiber-derived carbons. Int. J. Environ. Res. Public Health 20 (5), 4553.

Arya, S.S., Venkatram, R., More, P.R., Vijayan, P., 2022. The wastes of coffee bean processing for utilization in food: a review. J. Food Sci. Technol. 59 (2), 429–444. https://doi.org/10.1007/s13197-021-05032-5.

Asefaw, K.T., Bidira, F., Desta, W.M., Asaithambi, P., 2024. Investigation on pulsed-electrocoagulation process for the treatment of wet coffee processing wastewater using an aluminum electrode. Sustain. Chem. Environ. 6, 100085. https://doi.org/10.1016/j.scenv.2024.100085.

Ayeb, A., Binous, H., Dhaouadi, H., Dridi-Dhaouadi, S., 2024. Commercial Dimethoate Pesticide Adsorption on Organic Soil: Experimental and Theoretical Investigations. Chem. Africa 7 (10), 5521–5534.

Bakshi, P.S., Selvakumar, D., Kadirvelu, K., Kumar, N.S., 2020. Chitosan as an environment friendly biomaterial - a review on recent modifications and applications. Int. J. Biol. Macromol. 150, 1072–1083. https://doi.org/10.1016/j.ijbiomac.2019.10.113.

Bona, D., Bertoldi, D., Borgonovo, G., Mazzini, S., Ravasi, S., Silvestri, S., Zaccone, C., Giannetta, B., Tambone, F., 2023. Evaluating the potential of hydrochar as a soil amendment. Waste Manag. 159, 75–83. https://doi.org/10.1016/j.wasman.2023.01.024.

Cao, N., Ji, J., Li, C., Yuan, M., Guo, X., Zong, X., Li, L., Ma, Y., Wang, C., Pang, S., 2023. Rapid and efficient removal of multiple aqueous pesticides by one-step construction boric acid modified biochar [10.1039/D2RA07684E]. RSC Adv. 13 (13), 8765–8778. https://doi.org/10.1039/D2RA07684E.

Celis, R., HermosÍn, M.C., Cornejo, J., 2000. Heavy metal adsorption by functionalized clays. Environ. Sci. Technol. 34 (21), 4593–4599. https://doi.org/10.1021/es000013c.

Chen, X., Yao, X.-W., Diao, Y., Liu, H., Chen, M.-L., Feng, N.-J., Qian, W., Zhou, X.-H., Guo, P.-R., Kong, L.-J., Diao, Z.-H., 2024. Simultaneous removal of triadimefon and dinotefuran by a new biochar-based magnesium oxide composite in water: Performances and mechanism. Sep. Purif. Technol. 336, 126213. https://doi.org/10.1016/j.seppur.2023.126213.

Chiban, M., Soudani, A., Sinan, F., Persin, M., 2011. Single, binary and multi-component adsorption of some anions and heavy metals on environmentally friendly Carpobrotus edulis plant. Colloids Surf. B Biointerfaces 82 (2), 267–276. https://doi.org/10.1016/j.colsurfb.2010.09.013.

Da Mota, M.C.B., Batista, N.N., Rabelo, M.H.S., Ribeiro, D.E., Borém, F.M., Schwan, R.F., 2020. Influence of fermentation conditions on the sensorial quality of coffee inoculated with yeast. Food Res. Int. 136, 109482. https://doi.org/10.1016/j.foodres.2020.109482.

Dada, A.O., Olalekan, A.P., Olatunya, A.M., Dada, O., 2012. Langmuir, Freundlich, Temkin and Dubinin–Radushkevich Isotherms Studies of Equilibrium Sorption of Zn2+ Unto Phosphoric Acid Modified Rice Husk. IOSR J. Appl. Chem. 3, 38–45.

Dávila-Guzman, N.E., Cerino-Córdova, F.J., Diaz-Flores, P.E., Rangel-Mendez, J.R., Sánchez-González, M.N., Soto-Regalado, E., 2012. Equilibrium and kinetic studies of ferulic acid adsorption by Amberlite XAD-16. Chem. Eng. J. 183, 112–116. https://doi.org/10.1016/j.cej.2011.12.037.

De Jager, M., Schröter, F., Wark, M., Giani, L., 2022. The stability of carbon from a maize-derived hydrochar as a function of fractionation and hydrothermal carbonization temperature in a Podzol. Biochar 4 (1), 52. https://doi.org/10.1007/s42773-022-00175-w.

De Queiroz, V.T., Azevedo, M.M., da Silva Quadros, I.P., Costa, A.V., do Amaral, A.A., Juvanhol, R.S., de Almeida Telles, L.A., dos Santos, A.R., 2018. Environmental risk assessment for sustainable pesticide use in coffee production. J. Contam. Hydrol. 219, 18–27. https://doi.org/10.1016/j.jconhyd.2018.08.008.

Dong, X., Chu, Y., Tong, Z., Sun, M., Meng, D., Yi, X., Gao, T., Wang, M., Duan, J., 2024. Mechanisms of adsorption and functionalization of biochar for pesticides: a review. Ecotoxicol. Environ. Saf. 272, 116019. https://doi.org/10.1016/j.ecoenv.2024.116019.

Duran, J.E., Bayarri, B., Sans, C., 2024. Taguchi optimisation of the synthesis of vine-pruning-waste hydrochar as potential adsorbent for pesticides in water. Bioresour. Technol. 399, 130552.

Dutta, S., Gupta, B., Srivastava, S.K., Gupta, A.K., 2021. Recent advances on the removal of dyes from wastewater using various adsorbents: a critical review. Mater. Adv. 2 (14), 4497–4531. https://doi.org/10.1039/d1ma00354b.

Ebelegi, A.N., Ayawei, N., Wankasi, D., 2020. Interpretation of adsorption thermodynamics and kinetics. Open J. Phys. Chem. 10 (3), 166–182.

Elliott, H., Huang, C., 1979. The effect of complex formation on the adsorption characteristics of heavy metals. Environ. Int. 2 (3), 145–155. https://doi.org/10.1016/0160-4120(79)90072-2.

Elnour, A.Y., Alghyamah, A.A., Shaikh, H.M., Poulose, A.M., Al-Zahrani, S.M., Anis, A., Al-Wabel, M.I., 2019. Effect of pyrolysis temperature on biochar microstructural evolution, physicochemical characteristics, and its influence on biochar/polypropylene composites. Appl. Sci. 9 (6), 1149. https://doi.org/10.3390/app9061149.

Esquivel, P., Jimenez, V.M., 2012. Functional properties of coffee and coffee by-products. Food Res. Int. 46 (2), 488–495. https://doi.org/10.1016/j.foodres.2011.05.028.
Figueroa Campos, G.A., Sagu, S.T., Saravia Celis, P., Rawel, H.M., 2020. Comparison of batch and continuous wet-processing of coffee: changes in the main compounds in beans, by-products and wastewater. Foods 9 (8), 1135. https://doi.org/10.3390/foods9081135.
Fruehwirth, M., Sbizzaro, M., Rosa, D.M., Sampaio, S.C., Reis, R.R. d, 2020. Adsorption of atrazine by biochars produced from byproducts of the wood industry. Eng. Agrícola 40 (6), 769–776. https://doi.org/10.1590/1809-4430-Eng.Agric.v40n6p769-776/2020.
Fu, M.-M., Mo, C.-H., Li, H., Zhang, Y.-N., Huang, W.-X., Wong, M.H., 2019. Comparison of physicochemical properties of biochars and hydrochars produced from food wastes. J. Clean. Prod. 236, 117637. https://doi.org/10.1016/j.jclepro.2019.117637.
Genanaw, W., Kanno, G.G., Derese, D., Aregu, M.B., 2021. Effect of wastewater discharge from coffee processing plant on river water quality, Sidama region, South Ethiopia. Environ. Health Insights 15, 11786302211061047. https://doi.org/10.1177/11786302211061.
Gomes, H., Bento, E., Tavares, M.D., Santos, Y., da Costa, J.G., do Nascimento, R., Salvestrini, S., Teixeira, R., 2025. Removal of azoxystrobin and deltamethrin from water using activated biochar from Moringa oleifera L. wood: synthesis, characterization, and adsorption study. Molecules 30 (13), 2757.
Hailemariam, F.A., Velmurugan, P., Selvaraj, S.K., 2021. Treatment of wastewater from coffee (coffea arebica) industries using mixed culture Pseudomonas florescence and Escherichia coli bacteria. Mater. Today. Proc. 46, 7396–7401. https://doi.org/10.1016/j.matpr.2020.12.1124.
Hamdaoui, O., Naffrechoux, E., 2007. Modeling of adsorption isotherms of phenol and chlorophenols onto granular activated carbon: Part I. Two-parameter models and equations allowing determination of thermodynamic parameters. J. Hazard. Mater. 147 (1-2), 381–394. https://doi.org/10.1016/j.jhazmat.2007.01.021.
Handiso, B., Pääkkönen, T., Wilson, B.P., 2024. Effect of pyrolysis temperature on the physical and chemical characteristics of pine wood biochar. Waste Manag. Bull. 2 (4), 281–287. https://doi.org/10.1016/j.wmb.2024.11.008.
Heidarinejad, Z., Dehghani, M.H., Heidari, M., Javedan, G., Ali, I., Sillanpää, M., 2020. Methods for preparation and activation of activated carbon: a review. Environ. Chem. Lett. 18 (2), 393–415. https://doi.org/10.1007/s10311-019-00955-0.
Ho, Y.-S., McKay, G., 1999. Pseudo-second order model for sorption processes. Process Biochem. 34 (5), 451–465.
Hoseini, M., Cocco, S., Casucci, C., Cardelli, V., Corti, G., 2021. Coffee by-products derived resources. A review. Biomass.. Bioenergy 148, 106009. https://doi.org/10.1016/j.biombioe.2021.106009.
Hwang, K.-J., Shim, W.-G., Kim, Y., Kim, G., Choi, C., Kang, S.O., Cho, D.W., 2015. Dye adsorption mechanisms in TiO 2 films, and their effects on the photodynamic and photovoltaic properties in dye-sensitized solar cells. Phys. Chem. Chem. Phys. 17 (34), 21974–21981.
Ibarra-Taquez, H.N., GilPavas, E., Blatchley, E.R., Gómez-García, M.-Á., Dobrosz-Gómez, I., 2017. Integrated electrocoagulation-electrooxidation process for the treatment of soluble coffee effluent: Optimization of COD degradation and operation time analysis. J. Environ. Manag. 200, 530–538. https://doi.org/10.1016/j.jenvman.2017.05.095.
IBI, 2024. Global Biochar Market Report 2023. I. B. I. a. U. B. Intitative.
ICO, 2023. Coffee Report and Outlook. International Coffee Organization. Issue.
Ijanu, E.M., Kamaruddin, M.A., Norashiddin, F.A., 2019. Coffee processing wastewater treatment: a critical review on current treatment technologies with a proposed alternative. Appl. Water Sci. 10 (1), 11. https://doi.org/10.1007/s13201-019-1091-9.
Iriondo-DeHond, A., Iriondo-DeHond, M., del Castillo, M.D., 2020. Applications of compounds from coffee processing by-products. Biomolecules 10 (9), 1219. https://doi.org/10.3390/biom10091219.
Janu, R., Mrlik, V., Ribitsch, D., Hofman, J., Sedláček, P., Bielská, L., Soja, G., 2021. Biochar surface functional groups as affected by biomass feedstock, biochar composition and pyrolysis temperature. Carbon Resour. Convers. 4, 36–46. https://doi.org/10.1016/j.crcon.2021.01.003.
Kalinke, C., Zanicoski-Moscardi, A.P., de Oliveira, P.R., Mangrich, A.S., Marcolino-Junior, L.H., Bergamini, M.F., 2020. Simple and low-cost sensor based on activated biochar for the stripping voltammetric detection of caffeic acid. Microchem. J. 159, 105380. https://doi.org/10.1016/j.microc.2020.105380.
Khamwichit, A., Dechapanya, W., Dechapanya, W., 2022. Adsorption kinetics and isotherms of binary metal ion aqueous solution using untreated venus shell. Heliyon 8 (6), e09610. https://doi.org/10.1016/j.heliyon.2022.e09610.
Khan, T.A., Saud, A.S., Jamari, S.S., Rahim, M.H.A., Park, J.-W., Kim, H.-J., 2019. Hydrothermal carbonization of lignocellulosic biomass for carbon rich material preparation: a review. Biomass.. Bioenergy 130, 105384. https://doi.org/10.1016/j.biombioe.2019.105384.
Laili, N., Indrasti, N., Wahyudi, D., 2022. Design of sustainable coffee processing wastewater treatment system using K-means clustering algorithm. IOP Conference Series Earth Environmental Science 1063, 012032. https://doi.org/10.1088/1755-1315/1063/1/012032.
Langmuir, I., 1917. The constitution and fundamental properties of solids and liquids. J. Frankl. Inst. 183 (1), 102–105. https://doi.org/10.1016/S0016-0032(17)90938-X.
Lawal, A.A., Hassan, M.A., Ahmad Farid, M.A., Tengku Yasim-Anuar, T.A., Samsudin, M.H., Mohd Yusoff, M.Z., Zakaria, M.R., Mokhtar, M.N., Shirai, Y., 2021. Adsorption mechanism and effectiveness of phenol and tannic acid removal by biochar produced from oil palm frond using steam pyrolysis. Environ. Pollut. 269, 116197. https://doi.org/10.1016/j.envpol.2020.116197.
Lee, Y.-G., Shin, J., Kwak, J., Kim, S., Son, C., Kim, G.-Y., Lee, C.-H., Chon, K., 2021. Enhanced adsorption capacities of fungicides using peanut shell biochar via successive chemical modification with KMnO4 and KOH. Separations 8 (4), 52.
Lehmann, J., Cowie, A., Masiello, C., Kammann, C., Woolf, D., Amonette, J., Cayuela, M.L., Camps Arbestain, M., Whitman, T., 2021. Biochar in climate change mitigation. Nat. Geosci. 14. https://doi.org/10.1038/s41561-021-00852-8.
Leite, S.A., Guedes, R.N.C., Santos, M.P. d, Costa, D.R. d, Moreira, A.A., Matsumoto, S.N., Lemos, O.L., Castellani, M.A., 2020. Profile of coffee crops and management of the neotropical coffee leaf miner, Leucoptera coffeella. Sustainability 12 (19), 8011. ⟨https://www.mdpi.com/2071-1050/12/19/8011⟩.
Lima, É.C., Adebayo, M.A., Machado, F.M., 2015. Kinetic and Equilibrium Models of Adsorption. In: Bergmann, In.C.P., Machado, F.M. (Eds.), Carbon Nanomaterials as Adsorbents for Environmental and Biological Applications. Springer International Publishing, pp. 33–69. https://doi.org/10.1007/978-3-319-18875-1_3.
Liu, L., Luo, X.-B., Ding, L., Luo, S.-L., 2019. 4 - Application of Nanotechnology in the Removal of Heavy Metal From Water. In. In: Luo, X., Deng, F. (Eds.), Nanomaterials for the Removal of Pollutants and Resource Reutilization. Elsevier, pp. 83–147. https://doi.org/10.1016/B978-0-12-814837-2.00004-4.
Liu, Y., Ying, D., Sanguansri, L., Cai, Y., Le, X., 2018. Adsorption of catechin onto cellulose and its mechanism study: Kinetic models, characterization and molecular simulation. Food Res. Int. 112, 225–232.
Mansoori, S.A.A., Reza, Z., Mohammad, H., Mohammad, M.S., Abolfazl, J., Sadegh, S., Akbar, E., 2022. HSS anions reduction combined with the analytical test of aqueous MDEA in South Pars gas complex. Nat. Gas. Ind. B 9 (3), 318–324. https://doi.org/10.1016/j.ngib.2022.06.004.
Merhi, A., Kordahi, R., Hassan, H.F., 2022. A review on the pesticides in coffee: usage, health effects, detection, and mitigation. Front Public Health 10, 1004570. https://doi.org/10.3389/fpubh.2022.1004570.
Milanković, V., Tasić, T., Brković, S., Potkonjak, N., Unterweger, C., Bajuk-Bogdanović, D., Pašti, I., Lazarević-Pašti, T., 2024. Spent coffee grounds-derived carbon material as an effective adsorbent for removing multiple contaminants from wastewater: a comprehensive kinetic, isotherm, and thermodynamic study. J. Water Process Eng. 63, 105507. https://doi.org/10.1016/j.jwpe.2024.105507.
Mobarak, M.B., Pinky, N.S., Mustafi, S., Chowdhury, F., Nahar, A., Akhtar, U.S., Quddus, M.S., Yasmin, S., Alam, M.A., 2024. Unveiling the reactor effect: a comprehensive characterization of biochar derived from rubber seed shell via pyrolysis and in-house reactor. RSC Adv. 14 (41), 29848–29859. https://doi.org/10.1039/d4ra05562d.
Mosquera-Vivas, C.S., Martinez, M.J., García-Santos, G., Guerrero-Dallos, J.A., 2018. Adsorption-desorption and hysteresis phenomenon of tebuconazole in Colombian agricultural soils: experimental assays and mathematical approaches. Chemosphere 190, 393–404. https://doi.org/10.1016/j.chemosphere.2017.09.143.
Mounia, A., Mandi, L., Ouazzani, N., 2009. Removal of organic pollutants and nutrients from olive mill wastewater by a sand filter. J. Environ. Manag. 90, 2771–2779. https://doi.org/10.1016/j.jenvman.2009.03.012.
Mukarunyana, B., Boman, C., Kabera, T., Lindgren, R., Fick, J., 2023. The ability of biochars from cookstoves to remove pharmaceuticals and personal care products from hospital wastewater. Environ. Technol. Innov. 32, 103391. https://doi.org/10.1016/j.eti.2023.103391.

Murthy, P.S., Madhava Naidu, M., 2012. Sustainable management of coffee industry by-products and value addition—a review. Resour. Conserv. Recycl. 66, 45–58. https://doi.org/10.1016/j.resconrec.2012.06.005.
NAEB, 2024. Annual report: Agricultural export performance 2023-2024. National Agricultural Export Development Board (Issue).
NISR, 2023. Fifth Rwanda Population and Housing Census, 2022. National Institute of Statistics of Rwanda (Issue).
Oginni, O., Singh, K., 2020. Influence of high carbonization temperatures on microstructural and physicochemical characteristics of herbaceous biomass derived biochars. J. Environ. Chem. Eng. 8 (5), 104169. https://doi.org/10.1016/j.jece.2020.104169.
Pagni, R., 2006. Modern Physical Organic Chemistry (Eric V. Anslyn and Dennis A. Dougherty). J. Chem. Educ. 83 (3), 387. https://doi.org/10.1021/ed083p387.
Pandey, A., Soccol, C.R., Nigam, P., Brand, D., Mohan, R., Roussos, S., 2000. Biotechnological potential of coffee pulp and coffee husk for bioprocesses. Biochem. Eng. J. 6 (2), 153–162. https://doi.org/10.1016/S1369-703X(00)00084-X.
Poltronieri, P., Rossi, F., 2016. Challenges in specialty coffee processing and quality assurance. Challenges 7 (2), 19. ⟨https://www.mdpi.com/2078-1547/7/2/19⟩.
Prahas, D., Kartika, Y., Indraswati, N., Ismadji, S., 2008. Activated carbon from jackfruit peel waste by H3PO4 chemical activation: Pore structure and surface chemistry characterization. Chem. Eng. J. 140 (1), 32–42. https://doi.org/10.1016/j.cej.2007.08.032.
Prelac, M., Palčić, I., Cvitan, D., Anđelini, D., Repajić, M., Ćurko, J., Kovačević, T.K., Goreta Ban, S., Užila, Z., Ban, D., Major, N., 2023. Biochar from grapevine pruning residues as an efficient adsorbent of polyphenolic compounds. Materials 16 (13), 4716. ⟨https://www.mdpi.com/1996-1944/16/13/4716⟩.
Rattan, S., Parande, A.K., Nagaraju, V.D., Ghiwari, G.K., 2015. A comprehensive review on utilization of wastewater from coffee processing. Environ. Sci. Pollut. Res. 22 (9), 6461–6472. https://doi.org/10.1007/s11356-015-4079-5.
Romero, E., Méndez, A., Moral-Rodríguez, A.I., Gascó, G., Nogales, R., 2025. Comparative efficiency of hydrochar and biochar from spent Pleurotus ostreatus substrate for removing ciprofloxacin from water. J. Water Process Eng. 69, 106707. https://doi.org/10.1016/j.jwpe.2024.106707.
Sathish, K., Saraswat, S., 2025. Screening and characterization of thermally modified biowaste-derived hydrochars for slow-release fertilizer for alkaline soil reclamation. Clean. Waste Syst. 11, 100257. https://doi.org/10.1016/j.clwas.2025.100257.
Satyam, S., Patra, S., 2024. Innovations and challenges in adsorption-based wastewater remediation: a comprehensive review. Heliyon 10 (9), e29573. https://doi.org/10.1016/j.heliyon.2024.e29573.
Singh, S., Kapoor, D., Khasnabis, S., Singh, J., Ramamurthy, P.C., 2021. Mechanism and kinetics of adsorption and removal of heavy metals from wastewater using nanomaterials. Environ. Chem. Lett. 19 (3), 2351–2381. https://doi.org/10.1007/s10311-021-01196-w.
Soetaredjo, F.E., Ismadji, S., Santoso, S.P., Ki, O.L., Kurniawan, A., Ju, Y.-H., 2013. Recovery of catechin and epicatechin from sago waste effluent: study of kinetic and binary adsorption isotherm studies. Chem. Eng. J. 231, 406–413.
Solomakou, N., Drosaki, A., Zamvrakidis, G., Goula, A.M., 2023. Adsorption of phenolic compounds from olive mill wastewaters on spent coffee grounds: isotherms, kinetics, and pure phenol adsorption. Biomass.. Convers. Biorefinery 13 (18), 16557–16567. https://doi.org/10.1007/s13399-023-04088-x.
Srikhaow, A., Chaengsawang, W., Kiatsiriroat, T., Kajitvichyanukul, P., Smith, S.M., 2022. Adsorption kinetics of imidacloprid, acetamiprid and methomyl pesticides in aqueous solution onto eucalyptus woodchip derived biochar. Minerals 12 (5), 528. ⟨https://www.mdpi.com/2075-163X/12/5/528⟩.
Srikhaow, A., Win, E.E., Amornsakchai, T., Kiatsiriroat, T., Kajitvichyanukul, P., Smith, S.M., 2023. Biochar derived from pineapple leaf non-fibrous materials and its adsorption capability for pesticides. ACS Omega 8 (29), 26147–26157.
Taghizadeh, S.F., Rezaee, R., Azizi, M., Giesy, J., Karimi, G., 2022. Polycyclic aromatic hydrocarbons mycotoxins and pesticides residues in coffee a probabilistic assessment of risk to health. Int. J. Environ. Anal. Chem. 104. https://doi.org/10.1080/03067319.2022.2036984.
Takashina, T.A., Leifeld, V., Zelinski, D.W., Mafra, M.R., Igarashi-Mafra, L., 2018. Application of response surface methodology for coffee effluent treatment by ozone and combined Ozone/UV. Ozone Science Engineering 40 (4), 293–304. https://doi.org/10.1080/01919512.2017.1417112.
Tan, X., Liu, Y., Zeng, G., Wang, X., Hu, X., Gu, Y., Yang, Z., 2015. Application of biochar for the removal of pollutants from aqueous solutions. Chemosphere 125, 70–85. https://doi.org/10.1016/j.chemosphere.2014.12.058.
Tang, Y., Alam, M.S., Konhauser, K.O., Alessi, D.S., Xu, S., Tian, W., Liu, Y., 2019. Influence of pyrolysis temperature on production of digested sludge biochar and its application for ammonium removal from municipal wastewater. J. Clean. Prod. 209, 927–936. https://doi.org/10.1016/j.jclepro.2018.10.268.
Tangmankongworakoon, N., 2019. An approach to produce biochar from coffee residue for fuel and soil amendment purpose. Int. J. Recycl. Org. Waste Agric. 8 (1), 37–44. https://doi.org/10.1007/s40093-019-0267-5.
Toczydlowski, A.J.Z., Slesak, R.A., Venterea, R.T., Spokas, K.A., 2023. Pyrolysis temperature has greater effects on carbon and nitrogen biogeochemistry than biochar feedstock when applied to a sandy forest soil. For. Ecol. Manag. 534, 120881. https://doi.org/10.1016/j.foreco.2023.120881.
Tong, Y., McNamara, P.J., Mayer, B.K., 2019. Adsorption of organic micropollutants onto biochar: a review of relevant kinetics, mechanisms and equilibrium. Environ. Sci. Water Res. Technol. 5 (5), 821–838.
Tran, T.H., Le, A.H., Pham, T.H., Nguyen, D.T., Chang, S.W., Chung, W.J., Nguyen, D.D., 2020. Adsorption isotherms and kinetic modeling of methylene blue dye onto a carbonaceous hydrochar adsorbent derived from coffee husk waste. Sci. Total Environ. 725, 138325. https://doi.org/10.1016/j.scitotenv.2020.138325.
Tsigkou, K., Demissie, B.A., Hashim, S., Ghofrani-Isfahani, P., Thomas, R., Mapinga, K.F., Kassahun, S.K., Angelidaki, I., 2025. Coffee processing waste: unlocking opportunities for sustainable development. Renew. Sustain. Energy Rev. 210, 115263. https://doi.org/10.1016/j.rser.2024.115263.
Vijayaraghavan, K., Balasubramanian, R., 2021. Application of pinewood waste-derived biochar for the removal of nitrate and phosphate from single and binary solutions. Chemosphere 278, 130361. https://doi.org/10.1016/j.chemosphere.2021.130361.
Villanueva-Rodríguez, M., Bello-Mendoza, R., Wareham, D.G., Ruiz-Ruiz, E.J., Maya-Treviño, M.L., 2014. Discoloration and organic matter removal from coffee wastewater by electrochemical advanced oxidation processes. Water Air Soil Pollut. 225 (12), 2204. https://doi.org/10.1007/s11270-014-2204-6.
Vinícius de Melo Pereira, G., Soccol, V.T., Brar, S.K., Neto, E., Soccol, C.R., 2017. Microbial ecology and starter culture technology in coffee processing. Crit. Rev. Food Sci. Nutr. 57 (13), 2775–2788. https://doi.org/10.1080/10408398.2015.1067759.
Wan, J., Feng, X., Li, B., Wang, M., Tang, X., Chen, J., Rong, J., Ma, S., Jiang, Y., Zhang, Z., 2024. Effects of carbonization temperature and time on the characteristics of carbonized sludge. Water Sci. Technol. 89 (9), 2342–2366. https://doi.org/10.2166/wst.2024.119.
Weber Jr, W.J., Morris, J.C., 1963. Kinetics of adsorption on carbon from solution. J. Sanit. Eng. Div. 89 (2), 31–59.
Wu, F.-C., Tseng, R.-L., Juang, R.-S., 2009. Initial behavior of intraparticle diffusion model used in the description of adsorption kinetics. Chem. Eng. J. 153 (1), 1–8. https://doi.org/10.1016/j.cej.2009.04.042.
Xiang, H., Dai, K., Kou, J., Wang, G., Zhang, Z., Li, D., Chen, C., Wu, J., 2023. Selective adsorption of ferulic acid and furfural from acid lignocellulosic hydrolysate by novel magnetic lignin-based adsorbent. Sep. Purif. Technol. 307, 122840.
Xu, S., Chen, J., Peng, H., Leng, S., Li, H., Qu, W., Hu, Y., Li, H., Jiang, S., Zhou, W., Leng, L., 2021. Effect of biomass type and pyrolysis temperature on nitrogen in biochar, and the comparison with hydrochar. Fuel 291, 120128. https://doi.org/10.1016/j.fuel.2021.120128.
Yamal-Turbay, E., Graells, M., Pérez-Moya, M., 2012. Systematic assessment of the influence of hydrogen peroxide dosage on caffeine degradation by the photo-fenton process. Ind. Eng. Chem. Res. 51 (13), 4770–4778. https://doi.org/10.1021/ie202256k.
Zayas Péerez, T., Geissler, G., Hernandez, F., 2007. Chemical oxygen demand reduction in coffee wastewater through chemical flocculation and advanced oxidation processes. J. Environ. Sci. 19 (3), 300–305. https://doi.org/10.1016/S1001-0742(07)60049-7.
Zhang, C., Zhang, Z., Zhang, L., Li, Q., Li, C., Chen, G., Zhang, S., Liu, Q., Hu, X., 2020. Evolution of the functionalities and structures of biochar in pyrolysis of poplar in a wide temperature range. Bioresour. Technol. 304, 123002. https://doi.org/10.1016/j.biortech.2020.123002.
Zhu, L., Zhu, J., Zuo, R., Xu, Q., Qian, Y., An, L., 2023. Identification of microplastics in human placenta using laser direct infrared spectroscopy. Sci. Total Environ. 856, 159060. https://doi.org/10.1016/j.scitotenv.2022.159060.